MJSAT

Malaysian Journal of Science and Advanced Technology

journal homepage: https://mjsat.com.my/

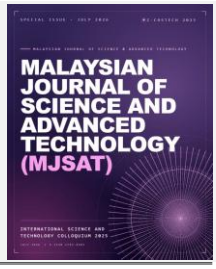

Structural, Electrical, Mechanical and Morphological Characterization of Methylcellulose–Magnesium Triflate (MgTf) Electrolyte Films with Deep Eutectic Solvent

Aiman Razi[1], Siti Zulaikha Mohd Yusof*[1], Muhammad Amin Asraff Kamarudin[1], Nuramirah Syafikah Mohd Soffian[1], and Nabilah Akemal Muhd Zailani[1]

[1]*Faculty of Applied Science, Universiti Teknologi MARA Cawangan Perlis, Kampus Arau, 02600, Arau, Malaysia.*

KEYWORDS

Solid polymer electrolyte
Methylcellulose
Magnesium Triflate
Deep eutectic solvent
Structural properties

ARTICLE HISTORY

Received 22 November 2025
Available online 21 August 2026

ABSTRACT

As an alternative to traditional liquid electrolytes, polymer electrolytes (PEs) have recently attracted attention, partly because they show high safety, sustainability in the environment, and design flexibility in new generation energy storage devices. The present research work is devoted to studying the structural, electrical, mechanical and morphological properties of the methylcellulose (MC)-based solid polymer electrolytes (SPEs) incorporation, enhanced with magnesium triflate (MgTf) as well as deep eutectic solvent (DES), choline chloride-1,3-propanediol) to have a complete picture of these kinds of SPEs properties. Distilled water was used as a solvent and the electrolytes were prepared through the solution casting technique using MgTf concentrations of 10, 30, and 50 wt. %, with constant DES content. Structural observations using the Fourier Transform Infrared Spectroscopy (FTIR) analysis showed a decrease in the crystallinity and increase in interactions of hydrogen bonding at broad O–H stretching region (around 3300–3500 cm^{-1}), which favors more mobility of ions in the presence of DES. These results were further confirmed by the electrochemical impedance spectroscopy (EIS) study which exhibited the highest ionic conductivity value of 6.06 x 10^{-6} Scm^{-1} in MC-MgTf(30)-DES sample. Optical microscopy also showed that the 30 wt.% MgTf-induced film structure was the most amorphous and homogeneous structure contributing to efficient transport paths of ions. According to the result obtained from tensile test, this composition provided high tensile strength of 6.70 MPa and elastic modulus of 197.73 MPa, which were a balance between flexibility and robustness. It can be concluded that the MC-MgTf(30)-DES formulation electrolyte performed the most advantageous combination of structural, electrical, mechanical and morphological properties.

1. INTRODUCTION

The increasing global demand for sustainable and efficient energy storage systems has intensified research efforts toward safer alternatives to conventional liquid electrolytes. Although liquid electrolytes exhibit high ionic conductivity, they suffer from inherent drawbacks such as flammability, leakage, and limited electrochemical stability, which raise serious safety and environmental concerns in applications including batteries and supercapacitors [1]. These limitations have accelerated the development of solid polymer electrolytes (SPEs) as safer and more mechanically robust alternatives.

SPEs offer improved safety, good mechanical integrity, and compatibility with flexible device architectures. In particular, biopolymer-based electrolytes have gained significant attention due to their biodegradability, renewability, and low toxicity. Among these materials, methylcellulose (MC), a cellulose derivative, has been widely investigated because of its excellent film-forming ability and environmental compatibility. However, the semi-crystalline nature of MC restricts polymer chain mobility, resulting in relatively low ionic conductivity and limited mechanical flexibility.

To overcome these limitations, the incorporation of suitable salts and plasticizers has been widely explored. Magnesium triflate (MgTf) serves as an effective ionic salt, providing mobile Mg^{2+} charge carriers while reducing polymer crystallinity. In addition, deep eutectic solvents (DES), such as

*Corresponding author:
E-mail address: Siti Zulaikha Mohd Yusof < sitizulaikhamy@uitm.edu.my >.
https://doi.org/10.56532/mjsat.v6iS1.790
2785-8901/

choline chloride/1,3-propanediol, function as green plasticizers that enhance polymer chain flexibility and disrupt strong intermolecular interactions, thereby promoting amorphous phase formation [2]. The increased amorphous content facilitates ion transport without compromising structural stability. Previous studies have demonstrated that salt and plasticizer incorporation can significantly influence either the ionic conductivity or mechanical properties of MC-based systems [3]. However, systematic investigations addressing both electrochemical and mechanical performance simultaneously remain limited.

Therefore, this study aims to comprehensively evaluate the structural, electrical, mechanical, and morphological properties of MC–MgTf–DES electrolyte films. By systematically varying the MgTf concentration, the optimal formulation is identified to achieve a balance between ionic conductivity, tensile strength, and amorphous characteristics. This work contributes to the development of environmentally friendly and mechanically stable polymer electrolytes suitable for next-generation magnesium-ion battery applications [4].

2. EXPERIMENTAL

2.1 Chemicals and Materials

Methylcellulose (MC, molecular weight: 88000 g mol^{-1}), and magnesium triflate ($Mg(CF_3SO_3)_2$, molecular weight: 322.44 g mol^{-1}, purity: 97%) were purchased from Sigma-Aldrich and used as received without further purification. Meanwhile, the DES with 1,3-propanediol and distilled water was prepared in the preliminary study. None of this compound were purified before usage.

2.2 Preparations of MC-MgTf-DES films

The MC-MgTf-DES polymer electrolyte films were prepared using the solution casting technique. In this method, 1 g of methylcellulose (MC) was dissolved in 50 mL of distilled water and stirred at room temperature until a clear solution was obtained. A fixed amount of deep eutectic solvent (choline chloride–1,3-propanediol, 1:2 molar ratio) which is 0.2 g was added as a plasticizer to all formulations. MgTf was incorporated at different weight percentages (10, 30 and 50 wt.%) relative to MC as shown as in Table 1. The mixtures were stirred until a uniform solution was achieved and subsequently cast into petri dishes (diameter: 90 mm). It also warrants high availability of mobile ions in the polymer by enhancing the dissociation of salts contained [5]. The films were dried at room temperature (25 °C) approximately 48 h, until complete solvent evaporation and formation of transparent polymer electrolyte films. For comparison, MC-DES films without MgTf were also prepared as control sample.

Table 1 tabulates the compositions of MC (in gram), DES (in gram), MgTf (in gram and weight percentage) for all samples designation. Figure 1 shows the homogeneity of all samples shows clear thin films.

Table 1. Compositions of MC–MgTf–DES SPEs

Designation	MC (g)	DES (g)	MgTf (g)	MgTf (wt.%)
MC-DES	1.00	0.2	0	0
MC-MgTf(10)-DES	1.00	0.2	0.10	10
MC-MgTf(30)-DES	1.00	0.2	0.30	30
MC-MgTf(50)-DES	1.00	0.2	0.50	50

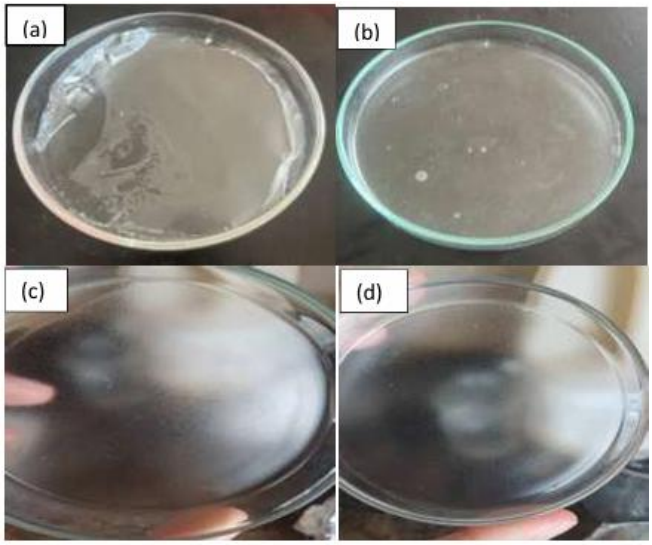

Fig. 1. Films of (a) MC-DES, (b) MC-MgTf(10)-DES, (c) MC-MgTf(30)-DES (d) MC-MgTf(50)-DES SPEs.

3. CHARACTERIZATIONS METHODS

3.1 Fourier Transforms Infrared Spectroscopy (FTIR)

To study structural properties of the polymer electrolyte films, Fourier Transform Infrared Spectrocopy (FTIR) was performed. Samples were loaded in the FTIR spectrometer and were scanned with wavenumber range of 4000-400 cm^{-1}. The resultant spectra gave the knowledge of vibrational modes of functional groups in the polymer, the salt and the deep eutectic solvent. This was analyzed to identify potential interaction of the components of electrolyte system, including the shift in the hydrogen bonding and coordination between the polymer and ionic salt. All these observations indicate that MgTf/DES addition not only altered the surrounding environment of MC but also induced the condition that led to the enhancement of ionic conductivity. Since FTIR sends infrared radiation about 10,000 – 100 cm^{-1} through a sample with some passed through and some radiation absorbed will converted into rotational and vibrational energy by sample molecules [6].

3.2 Electrochemical Impedance Spectroscopy (EIS)

Electrochemical impedance spectroscopy (EIS) is an important method to describe the electrochemical characteristics of polymer electrolytes. Measurements will be performed at room temperature using a HIOKI 35232- 01 LCR meter. Impedance was recorded across the frequency range of 100 Hz to 1 MHz, with a polymer electrolyte film placed between two stainless steel blocking electrodes. A micrometer screw gauge should be used to measure the thickness of the film before making the measurement. In three distinct regions of the films, the impedance was measured, and the average ionic conductivity of each sample was evaluated using Equation (1).

$$\sigma = \frac{l}{R_b.A} \quad (1)$$

Where, R_b is the bulk resistance (Ω), l is the thickness of the film (cm), and A is the effective contact area of the electrode and the electrolyte (cm^2). Wavenumber (cm^{-1})

3.3 Tensile Test

The Instron Universal Testing Instrument (3365, Instron USA) was used to assess the mechanical properties of the film samples (i.e., tensile strain, tensile stress, and Young's modulus). Each sample was cut into 1 cm x 7.0 cm pieces and tested at 5mm/min cross-speed according to ASTM D882. Two replicates were performed for each sample formulation.

3.4 Optical Microscopy (OM)

The morphology of the plasticized TSP-based electrolyte films was viewed using optical microscope (Olympus CX31 Microscope). 10x magnification was used to examine the materials.

4. Result and Discussion

4.1 Structural Properties Analysis of MC-based SPEs

FTIR was done to examine the compounds structural rapport, as well as molecule-molecule alterations in MC-MgTf-DES electrolyte scheme. The characteristic absorption bands and their assignments are summarized in Table 2.

Absorption in the range of 3300-3500 cm^{-1} was evidenced by the presence of a wide band of absorption due to O-H stretching vibrations of intermolecular hydrogen bonding in the polymer chains in the spectrum of neat MC [7]. Minor contributions from absorbed moisture may also be present due to the hygroscopic nature of the polymer and electrolyte system. However, all samples were prepared and characterized under consistent conditions.

When MgTf and DES were incorporated, this band broadened and shifted in peak position that indicated new hydrogen bond formation and the presence of less polymer-polymer interaction [8]. This change is indicative of incremented amorphous content in the system which is a key aspect in ionic transport.

Also, the C-O-C stretching vibrations of MC at 1050-1150 cm^{-1} were variable in terms of intensities and slightly displaced in position. These phenomena imply the coordination of the oxygen atoms of MC with the Mg^{2+} cations supplied by magnesium triflate, which further prove the presence of salt - polymer interactions. Specific absorption bands in spectra alleviated the presence of triflate anion (SO^{3-}) in 1000 to 1250 cm^{-1} region that confirmed the successful incorporation of MgTf within a polymer matrix.

Figure 2 presents the FTIR spectra of MC–DES polymer electrolyte films containing 0, 10, 30, and 50 wt.% MgTf. The incorporation of DES induces noticeable structural modifications within the polymer matrix. Strong hydrogen bonding interactions between DES molecules and the hydroxyl groups of methylcellulose disrupt the ordered arrangement of the polymer chains, leading to a reduction in crystallinity and the development of a more flexible and amorphous structure [13,14].

Table 2. FTIR wavenumbers and vibrational mode assignments of MC–DES–MgTf SPEs system.

Wave number (cm^{-1})/ Type of Vibration	MC-DES	MC-MgTf10-DES	MC-MgTf30-DES	MC-MgTf50-DES	DES Effect	Note
~3400 (O–H Stretching) [7]	Broad	Broader	Very broad	Very Broad	Increased	Hydrogen bonding enhanced, increased amorphous character
~2900 (C–H Stretching) [9]	Present	Stable	Stable	Stable	No major change	Backbone aliphatic chains remain intact
1650–1750 (C=O Stretching) [10]	Present	Present	Strong	Strong	Visible	Interaction between DES / MgTf and MC oxygen sites
1250–1050 (S=O / C–O–C Stretching) [11]	Sharp	Sharper	Sharpest	Sharpest	Increased	Salt dissociation and ether group involvement enhanced
~1000 (C–O Stretching) [12]	Increased	Strong	Stronger	Strongest	Enhance	Ion mobility and backbone flexibility increased

Such structural disorder is beneficial for ionic conduction, as the increased amorphous content enhances free volume and promotes greater segmental mobility of the polymer chains. These factors facilitate ion transport within the matrix, thereby contributing to the improvement in ionic conductivity observed in the electrolyte system.

The FTIR data overall showed that MgTf and DES together acted synergistically to modifying the structural environment of MC, decreasing crystallinity, and increasing interaction between polymers and salts plasticizers. Such changes provided positive environment to ionic conduction and justified the results made in conductivity tests.

4.2 Ionic Conductivity-Electrical Properties Analysis of MC-based SPEs

Electrochemical impedance spectroscopy technique applies a sinusoidal voltage or current to the electrochemical cell, and it can be used to determine complex impedance as a function of frequency by measuring the current and voltage that occur [15]. EIS works very effectively to explain charge transfer and ionic conductivity in polymer electrolytes. Ohmic resistance, charge transfer resistance, and mass transport limits are just a few of the electrochemical processes that it might draw attention to comprehend how well polymer electrolytes function in devices like batteries and supercapacitors [16,17].

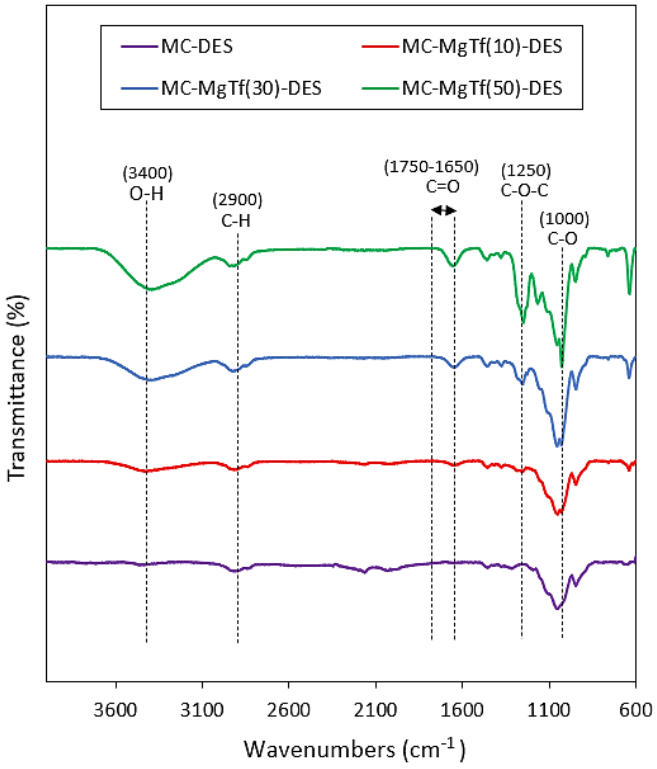

Fig. 2. FTIR spectra of MC-DES, MC-MgTf(10)-DES, MC-MgTf(30)-DES, MC-MgTf(50)-DES SPEs

According to Zhu et al. [18], the adaptability of EIS allows it to be applied to a variety of electrochemical systems that can provide valuable insights into the dynamics of ion transport and the effects of different dopants on conductivity. The electrical properties of MC-based polymer electrolyte films doped with varying amounts of magnesium triflate was analyzed using EIS technique, specifically on ionic conductivity study. The ionic conductivity influenced by number of charge carriers and its mobility within polymer matrix while for low concentration of MgTf may result in insufficient ion availability, an excessive concentration could lead to ion aggregation and a reduction in conductivity due to ion pairing and phase separation [19]. Besides, EIS is employed to evaluate ionic conductivity of various MC-DES-MgTf compositions allowing for determination of concentration that yields.

Figure 3 shows the Cole-Cole (Nyquist) plots for selected samples. The MC-DES sample displayed a well-defined semicircle in the high-frequency region, indicating high bulk resistance (R_b) and low ion mobility [20]. In contrast, DES and MgTf-doped samples, particularly at higher salt concentrations, showed reduced semicircle diameters and the appearance of a low frequency spike, signifying improved ion transport and electrode electrolyte interfacial polarization. Figure 3 shows Cole-cole plot of MC-DES, MC-MgTf(10)-DES, MC-MgTf(30)-DES and MC-MgTf(50)-DES samples. The plot in Figure 3 (a) exhibits a very large semicircle at high frequencies, followed by a faint, incomplete tail at low frequencies. The relatively larger diameter of the semicircle suggests higher bulk resistance and lower ionic conductivity compared to graph in Figure 3 (b) that contained 10 wt.% of MgTf which indicating better performance of electrolyte in this sample. As for Figure 3 (c), it had smaller semicircle and a sharper vertical tail indicates lower resistance and enhance the ionic conductivity. This behaviour is associate with the MC-MgTf(30)-DES sample which showed the highest conductivity in the experimental results.

The combination of low resistance with clear diffusion tail confirms the optimal ion dissociation and efficient ion transport. The Nyquist plot of graph (d) in Figure 3 shows a moderate semicircle followed by a visible tail. Despite its higher salt content, MC-MgTf(50)-DES sample may suffer from ion aggregation and increased viscosity which reducing its conductivity.

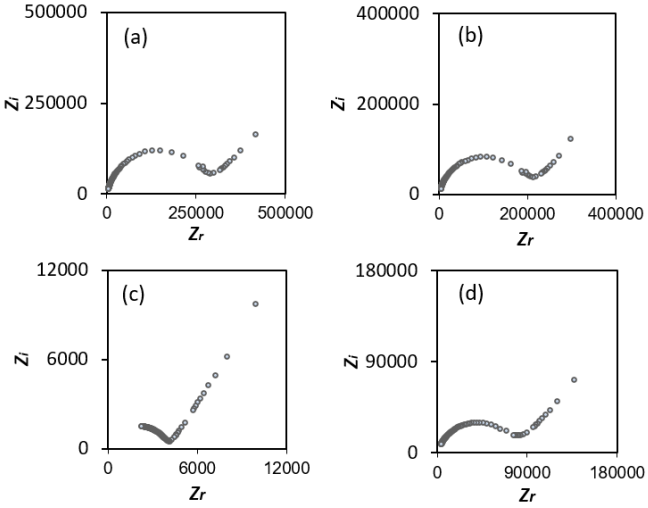

Fig. 3. Cole-Cole plots for (a) MC-DES, (b) MC-MgTf(10)-DES, (c) MC-MgTf(30)-DES (d) MC-MgTf(50)-DES electrolyte samples.

Table 3 presents the measured bulk resistances and conductivity values for each sample composition. Based on the data presented in Table 2, the MC-DES sample recorded bulk resistance of 2.723×10^5 Ω which gave an ionic conductivity of 7.89×10^{-8} S.cm^{-1}, indicating the role of DES in increasing polymer flexibility and chain mobility. The MC-DES sample without salt exhibited very low conductivity in the range of 10^{-8} S.cm^{-1}, indicating that DES alone is insufficient to provide adequate ionic mobility. Upon the addition of 10 wt.% MgTf, the R_b value decreased to 2.143×10^5 Ω which contributed to the enhancement of conductivity value to 6.67×10^{-7} S.cm^{-1}, suggesting that the salt successfully introduced the free ions (Mg^{2+} and $CF_3SO_3^-$) into the polymer matrix.

The highest conductivity was recorded at 30 wt.% MgTf composition with exhibited R_b and ionic conductivity values of 4.133×10^3 Ω and 6.06×10^{-6} S.cm^{-1}, respectively. This leading to a significant rise in ionic conductivity due to a higher number of dissociated charge carriers. This composition benefited from sufficient ion availability without experiencing significant ion pairing or aggregation. However, with further addition of 50 wt.% MgTf, the trend shows the increment of bulk resistance value again to 8.017×10^4 Ω with conductivity decreased to 2.73×10^{-7} S.cm^{-1}, likely due to ion clustering, increased viscosity, or reduced segmental motion within the matrix [21].

These findings demonstrate a clear trend of ionic conductivity increases with the inclusion of DES and MgTf, peaking around 10–30 wt. % salts loading. The combined effect of ion dissociation and polymer chain mobility optimization enhances the electrochemical performance of MC based films.

Table 3. Bulk resistance and ionic conductivity of MC-DES, and MC-DES-MgTf 10-50 wt.%.

Designation	Bulk Resistance (Ω)	Ionic Conductivity, σ ($S.cm^{-1}$)
MC-DES	2.723×10^5	7.89×10^{-8}
MC-MgTf(10)-DES	2.143×10^5	6.67×10^{-7}
MC-MgTf(30)-DES	4.133×10^3	6.06×10^{-6}
MC-MgTf(50)-DES	8.017×10^4	2.73×10^{-7}

Figure 4 illustrates the variation in ionic conductivity of all samples based on the data presented in Table 2. As observed, the conductivity increases with increasing MgTf content, reaching a maximum at 30 wt.%, which represents the optimum salt concentration. This enhancement is attributed to the increased number of free charge carriers resulting from effective salt dissociation within the polymer matrix.

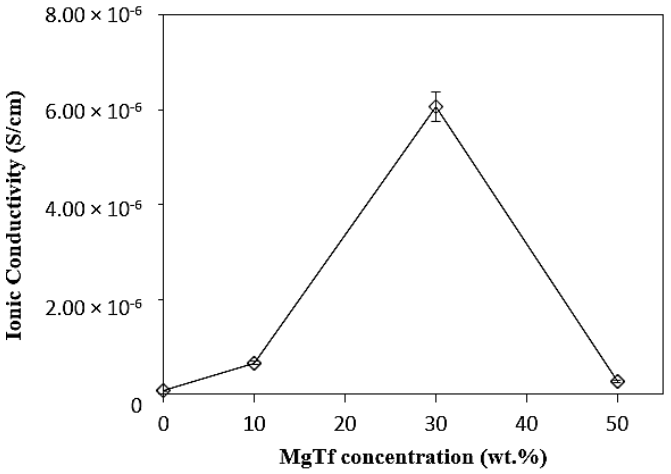

Fig. 4. Variation of ionic conductivity with MgTf concentration in MC–MgTf–DES SPE films.

However, a further increase to 50 wt.% MgTf leads to a decline in conductivity. This reduction is likely due to ion pairing and salt aggregation effects beyond the optimum concentration, which limit the mobility of charge carriers. The optimum composition reflects a balanced interaction between the polymer host and the dissolved salt, resulting in the highest achievable ionic conductivity.

4.3 Mechanical Properties Analysis of MC-based SPEs

Table 4 shows the Young's modulus and stress achieved by all specimens. As shown in the Table 3, the Young's modulus, which indicates material stiffness, shows a clear trend of MC-MgTf(30)-DES sample exhibits the highest modulus at 197.73 MPa, indicating a significantly stiffer and more rigid polymer matrix compared to the other samples. This suggests that the addition of 30 wt.% MgTf leads to strong ionic interactions and improved packing within the polymer structure. MC-MgTf(10)-DES and MC-DES samples have moderate modulus values of 79.02 MPa and 43.20 MPa respectively, while MC-MgTf(50)-DES sample records the lowest modulus at 30.17 MPa, reflecting a softer and more flexible material due to excessive salt loading that disrupts polymer chain packing [22]. In terms of tensile stress (σ), MC-DES sample achieves the highest value of 8.91 MPa, followed closely by MC-MgTf(10)-DES at 8.40 MPa. This aligns with their relatively lower flexibility and brittle nature, which enables them to resist higher stress before breaking [19]. Meanwhile, MC-MgTf(30)-DES and MC-MgTf(50)-DES samples exhibit lower stress values of 6.70 MPa and 4.94 MPa, respectively, consistent with their more ductile behavior. The results suggest that while MC-MgTf(30)-DES sample has the highest stiffness, its stress-bearing capacity is slightly compromised due to increased flexibility [23]. Overall, these findings highlight the trade-off between stiffness, strength, and ductility in polymer electrolyte design, with MC-MgTf(30)-DES sample offering the most balanced mechanical performance.

Table 4. Young modulus-stress of MC-MgTf-DES SPEs

Designation	Young Modulus (MPa)	Stress, σ
MC-DES	43.20	8.91
MC-MgTf(10)-DES	79.02	8.40
MC-MgTf(30)-DES	197.73	6.70
MC-MgTf(50)-DES	30.17	4.94

Figure 5 (a) shows the data of tensile test results for the MC-DES provide insight into its mechanical behavior under load. Results were obtained for sample that measured exactly the same which is 10 mm wide and 0.1077 mm thick. Specimen reached only 9.61 N during testing. Correlating with this, the computed stresses at maximum load were found to be 8.91 MPa for specimen. The strain at the fracture point reached zero for specimen, showing that the cracking occurred very quickly once the highest stress was applied. It means the material can fail without a visible neck or much plastic deformation [24].

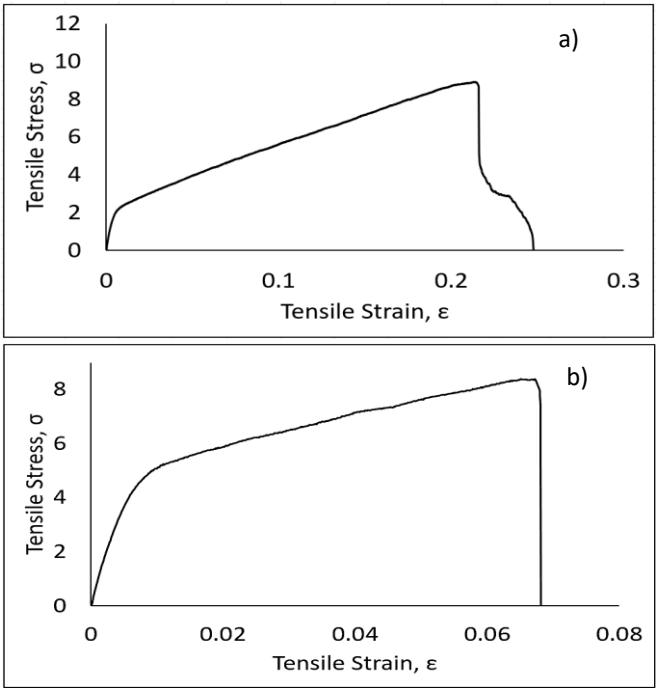

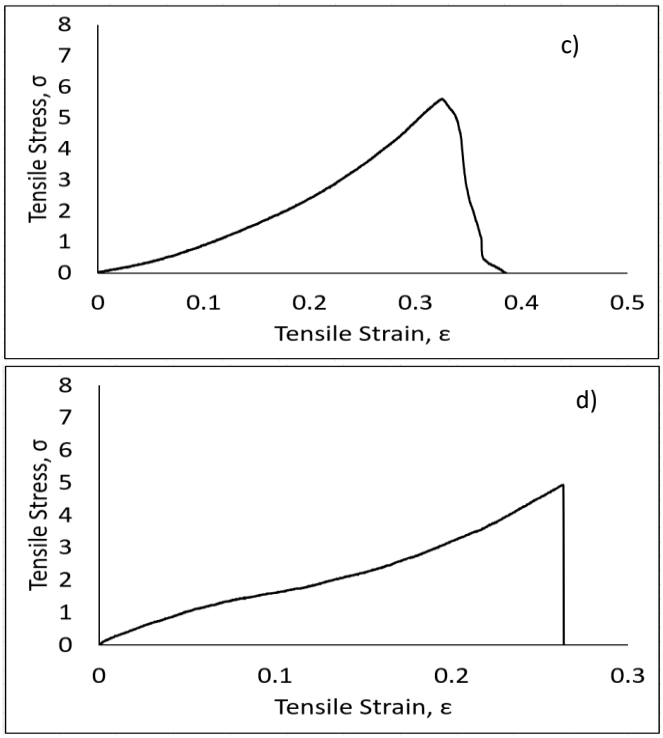

Fig. 5. A stress-strain graph for tensile testing result of specimen a) MC-DES, b) MC-MgTf(10)-DES, c) MC-MgTf(30)-DES and d) MC-MgTf(50)-DES electrolytes

The Young's modulus of the specimen is 43.20 MPa, suggesting that there were some differences in the material or the samples' uniformity. Even so, the specimens became elongated by over 20% under maximum load and further deformed more than 23% before failing, demonstrating that the material can tolerate significant strain. All in all, MC-DES is a good ductile material, though its tensile strength and stiffness are generally low and can change somewhat from sample to sample.

Figure 5 (b) shows the data of tensile test result for MC-MgTf(10)- DES that is shown to have low mechanical strength and stiffness when tested under tension. The specimen was 10 mm width and 0.10630 mm thickness, the specimen did which carried 8.92 N which low than specimen MC-DES. Modest stiffness was found, since young's modulus for the specimen measured 79.02 MPa. At the maximum load, the specimen experienced 8.40 MPa tensile stress. Greater ductility was shown by the specimen, as its strain at maximum load was higher (6.51%). The outcome from specimen suggests that they broke without plastic deformation. According to the result, this sample has modest strength and medium ductility and there is slight variability among the specimens.

Figure 5 (c) shows the data of tensile test results for MC-MgTf(30)- DES. The results of the tensile test indicate that specimens exhibit unique mechanical characteristics. The samples which each had the same dimensions 70 mm x 10 mm x 0.1034 mm, showed different levels of strength and ductility. The specimen was stronger and stiffer, achieving a maximum load of 6.93 N and a tensile stress of 6.70 MPa compared to specimens above. This specimen was able to sustain only 5.81 N of maximum load and 6.70 MPa of tensile stress, while having a modulus of 197.73 MPa, so it was stiffer. This specimen had much greater ductility, holding up to 38.41% of total deformation before tearing and experiencing a maximum load of 32.46%. The increase in Young's modulus suggests enhanced intermolecular interactions between Mg^{2+} ions and the hydroxyl groups of methylcellulose. These interactions restrict polymer chain mobility and improve structural rigidity [25]. All in all, the specimen of MC-MgTf(30)-DES electrolyte was stronger and stiffer than other specimens.

Figure 5 (d) shows the data of tensile test results for MC-MgTf(50)-DES, both specimens had same dimensions which is 10 mm wide and 0.1064 mm thick, resulted in different tensile test values for strength, stiffness and consistency. This specimen highest load was 5.25 N and maximum stress was 4.94 MPa. This demonstrates that this specimen took more effort to break before failing. In addition, the specimen had a modulus of elasticity of 30.17 MPa which means it can tolerate much more stress without as much deformation. Although it varied in stiffness, specimens showed a significant ability to elongate during the test. When tested, the tensile strain of the specimen attained tensile strain of 26.32% at maximum load and 26.34% at break. The large strains at fracture mean the test could elongate a lot before breaking which suits uses where being flexible and absorbing a lot of energy is important [26]. At higher MgTf content, Young's modulus decreases, indicating increased plasticization and reduced intermolecular cohesion. The incorporation of DES disrupts hydrogen bonding within the polymer matrix, increases amorphous content, and enhances chain mobility, leading to a softer and more flexible film.

Based on the tensile test results, sample of MgTf with 30 wt. % demonstrates better overall mechanical performance compared to sample with no addition of MgTf, 10 and 50 wt. % of MgTf composition. The MC-MgTf(30)-DES sample have greater maximal loads (up to 6.93 N) and tensile stresses (up to 6.70 MPa) and quite stronger stiffness (up to 197.73 MPa). However, though both MC-MgTf(30)-DES and MgTf50 samples showed promising results in ductility, the former left a greater balance between strength and flexibility. Comparatively, MC-MgTf(50)-DES sample possessed very low levels of strength (maximum loading only up to 5.25 N) and very low level of stiffness (maximum modulus only 30.17 MPa) although the product had good elongation. Lastly, the performance of MC-MgTf(30)-DES samples was more similar across specimens as compared to MC-MgTf(50)-DES samples which exhibited more variations, with one specimen. Thus, the sample of MC MgTf(30)-DES is a more viable material, all-round, as it has stronger strength and stiffness, is reliable and has ductility, and hence may be more applicable in a structural or load-bearing system.

4.4 Morphological Properties Analysis of MC-based SPEs

Optical microscopy provides insight into the surface uniformity and dispersion of MgTf within the polymer matrix, allowing correlation between morphological features and the observed electrical and mechanical properties. Figure 6 displays the optical micrographs of (a) MC–DES, (b) MC–MgTf (10 wt.%), (c) MC–MgTf (30 wt.%), and (d) MC–MgTf (50 wt.%) polymer electrolyte films.

The morphology of MC-DES SPEs shows small microstructural parts is shown in Figure 6 (a). The film is in overall smooth and steady impression showing excellent film-forming power and even combination of components. On a

closer look however, one can see fine variations in texture at the surface and scattered bright and dark areas. The characteristics can represent concentrated salt rich areas, tiny crystalline clusters of MgTf through solvent evaporation. It would seem that the dispersion of the salt as well as the plasticization of the polymer network is reinforced by the presence of the deep eutectic solvent and distilled water resulting in decreased phase separation at a large scale and instead creating homogeneous films [27]. Still, the presence of small inhomogeneities which can still be observed at such magnification signifies the presence of small clusters, which might affect the mechanical properties.

The images provided under the microscope show the morphology of the surface of solid polymer electrolytes that contain MC-DES with different concentrations of MgTf. These images play crucial roles in the explanation of the structural impacts of salt inclusion into polymer matrix. When the amount of 10 wt.% of MgTf is added as shown in Figure 6 (b), there are some modifications in the surface morphology. Many granular and dark, circular to rod-like objects are observed, which means that there is the presence of salt crystallites in the matrix [28]. This implies that the salt is not being dissolved completely and blending with the MC thus leading to phase separation and heterogeneous regions. Although ionic content is added, there is the possibility of build-up of undissolved salt particles resulting in ionic clogging with decreased movement of viable ions.

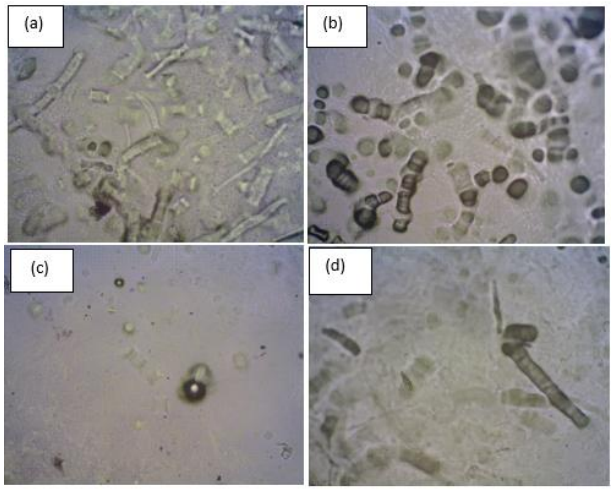

Fig. 6. Optical micrographs for (a) MC-DES, (b) MC-MgTf 10, (c) MC-MgTf 30, (d) MC-MgTf 50 electrolyte films

At MC-MgTf(30)-DES sample as shown in Figure 6 (c), the morphology is turned to a much more homogeneous and amorphous structure. The surface looks smoother and there are smaller crystallites or aggregates of salt that could be observed. That means better interaction and compatibility of MC and MgTf, and, the salt gets better integrated in the polymer matrix. It is a much-preferred amorphous phase in polymer electrolytes because this usually improves segmental mobility in the polymer chains and promotes easier ionic transport because of lower crystallinity [29].

Lastly, MC-MgTf(50)-DES sample as shown as Figure 6 (d) causes the reappearance of uneven and bulky forms, consisting of fibrous as well as granular shapes. The polymer matrix is disrupted again implying that the polymer is overloaded with salt such that it is not able to absorb and distribute it equally. This causes recrystallization of salt rich domains and may result in poor dispersion of ions that affects the mechanical and electrochemical behaviours of electrolyte negatively.

Among the four samples, the MC-MgTf(30)-DES sample shows the most optimal morphology for solid polymer electrolyte applications. Smooth amorphous surface is an indication of intense salt-polymer interaction, good dispersion of salt and low crystallinity which acts to improve mechanical stability. Thus, samples with absence of MgTf and presence of 10 and 50 wt.% of MgTf contents shows significant issues such as inefficient dispersion or saturation. Therefore, a quantity of MC-MgTf(30)-DES is optimal in terms of combining structural stability and electrochemical active performance.

5. CONCLUSION

The use of biodegradable methylcellulose (MC) and environmentally friendly deep eutectic solvent (DES) along with non-rare magnesium triflate (MgTf) revelation indicates that there is a possible and promising substitute to the traditional liquid and synthetic polymer electrolytes. Out of all the examined compositions, 30 wt.% MgTf was the best in terms of overall performance. The FTIR results showed that the crystallinity decreased and hydrogen bonding interactions were stronger in the broad OH region (3300-3500 cm^{-1}) which is an indication of better polymer ion interactions and higher ion mobility with the presence of DES. These results were validated by electrochemical impedance spectroscopy (EIS) with the highest ionic conductivity being 6.06×10^{-6} S cm^{-1} using the MC-DES system and this value greatly increased when MgTf was introduced with a significant increase at 30 wt.%. Tensile testing also proved that there was a good balance between the mechanical strength and the flexibility of the material tensile strength was 6.70 MPa, and the elastic modulus was 197.73 Mpa. The uniform and mainly amorphous structure of the 30 wt.% MgTf film allowed a good passage of ions. In general, this optimized MC -MgTf-DES electrolyte is able to address several important weaknesses of bio-based hosts and it has high potential to be used in magnesium-ion batteries, supercapacitors, and other sustainable solid-state energy storage systems.

REFERENCES

[1] Rao, A., Bhat, S., De, S., & Cyriac, V. (2024). Improving supercapacitor performance with novel potato starch-PVA solid polymer electrolyte blend modified by sodium perchlorate-glycerol additives. Journal of Energy Storage, 102. doi: https://doi.org/10.1016/j.est.2024.113965

[2] Veurink, M., Koster, M., & Berg, L. T. W. de J. den. (2023). The history of DES, lessons to be learned. Pharmacy World & Science : PWS, 27(3), 139–143. doi: https://doi.org/10.1007/s11096-005-3663-z

[3] Murali, A., Ramesh, R., Sakar, M., Park, S. J., & Han, S. S. (2024). Unveiling the potential of emergent nanoscale composite polymer electrolytes for safe and efficient all solid-state lithium-ion batteries. In RSC Advances (Vol. 14, Issue 42, pp. 30618–30629). Royal Society of Chemistry. doi: https://doi.org/10.1039/D4RA05134C

[4] Aziz, S. B., Asnawi, A. S. F. M., Kadir, M. F. Z., Alshehri, S. M., Ahamad, T., Yusof, Y. M., & Hadi, J. M. (2021). Structural, electrical and electrochemical properties of glycerolized biopolymers based on chitosan (Cs): Methylcellulose (mc) for energy storage application. Polymers, 13(8). doi: https://doi.org/10.3390/polym13081183

[5] Barbosa, J. C., Gonçalves, R., Costa, C. M., & Lanceros-Méndez, S. (2022). Toward Sustainable Solid Polymer Electrolytes for Lithium-Ion Batteries. In ACS Omega (Vol. 7, Issue 17, pp. 14457–14464). American Chemical Society. doi: https://doi.org/10.1021/acsomega.2c01926

[6] RTI Laboratories. (2025). FTIR analysis. Rtilab.com. url: https://rtilab.com/techniques/ftir-analysis/

[7] Doumani, J., Zahn, K., Yu, S., Barrios, G. R., Sasmal, S., Kikuchi, R., & Kono, J. (2023). Macroscopically self-aligned and chiralized carbon nanotubes: From filtration to innovation. arXiv preprint. doi: https://doi.org/10.48550/arXiv.2312.00984

[8] Kiruthika, S., Malathi, M., & Selvasekarapandian, S. (2024). Study of pectin based biopolymer electrolytes with magnesium triflate (MgTf2) for applications in magnesium batteries. Ionics, 30(9), 5237–5251. doi: https://doi.org/10.1007/s11581-024-05690-3

[9] Nayak, P., Sudhakar, Y. N., De, S., Ismayil, & Shetty, S. K. (2023). Optimization of Chitosan: Methylcellulose polyblend to obtain highly amorphous polymer matrix useful for ion transportation. Indian Journal of Physics, 97(12), 3483–3493. doi: https://doi.org/10.1007/s12648-023-02684-1

[10] Nofal, M. M., Aziz, S. B., Brza, M. A., Abdullah, S. N., Dannoun, E. M. A., Hadi, J. M., Murad, A. R., Al-Saeedi, S. I., & Kadir, M. F. Z. (2022). Studies of Circuit Design, Structural, Relaxation and Potential Stability of Polymer Blend Electrolyte Membranes Based on PVA:MC Impregnated with NH4I Salt. Membranes, 12(3), 284. doi: https://doi.org/10.3390/membranes12030284

[11] Oliveira, R. L., Vieira, J. G., Barud, H. S., Assunção, R. M. N., Filho, G. R., Ribeiro, S. J. L., & Messadeqq, Y. (2015). Synthesis and Characterization of Methylcellulose Produced from Bacterial Cellulose under Heterogeneous Condition. *Journal of the Brazilian Chemical Society*. doi: https://doi.org/10.5935/0103-5053.20150163

[12] Faris, B. K., Hassan, A. A., Aziz, S. B., Brza, M. A., Abdullah, A. M., Abdalrahman, A. A., Ali, O. a. A., & Saleh, D. I. (2021). Impedance, electrical Equivalent circuit (EEC) modeling, structural (FTIR and XRD), dielectric, and electric modulus study of MC-Based Ion-Conducting solid polymer electrolytes. *Materials*, *15*(1), 170. doi: https://doi.org/10.3390/ma15010170

[13] Kumar, D., Mukherjee, S., & Das, A. (2024). Effect of NASCION-Type ceramic dispersion in PAN/PVA-based blend polymer electrolyte: A structural, thermal, and electrical study. Journal of Applied Polymer Science, 141(25). doi: https://doi.org/10.1002/app.55552

[14] Meng, N., Zhu, X., & Lian, F. (2022). Particles in composite polymer electrolyte for solid-state lithium batteries: A review. Particuology, 60, 14–36. doi: https://doi.org/10.1016/j.partic.2021.04.002

[15] Juang, L., Kollmeyer, P., Zhao, R., Jahns, T., & Lorenz, R. (2024). The impact of dc bias current on the modeling of lithium iron phosphate and lead acid batteries observed using electrochemical impedance spectroscopy. doi: https://doi.org/10.1109/ecce.2014.6953745

[16] Zheng, Z., Petrone, R., Péra, M., Hissel, D., Becherif, M., & Pianese, C. (2023). Diagnosis of a commercial pem fuel cell stack via incomplete spectra and fuzzy clustering doi: https://doi.org/10.1109/iecon.2013.6699371

[17] Chang, B. and Park, S. (2021). Electrochemical impedance spectroscopy. Annual Review of Analytical Chemistry, 3(1), 207-229. doi: https://doi.org/10.1146/annurev.anchem.012809.102211

[18] Zhu, S., Sun, X., Gao, X., Wang, J., Zhao, N., & Sha, J. (2022). Equivalent circuit model recognition of electrochemical impedance spectroscopy via machine learning. Journal of Electroanalytical Chemistry, 855, 113627 doi: https://doi.org/10.1016/j.jelechem.2019.113627

[19] Wang, G. Y., Lian, K., & Chu, T. (2021). Electrolyte-Gated Field Effect Transistors in Biological sensing: A survey of electrolytes. IEEE Journal of the Electron Devices Society, 9, 939–950. doi: https://doi.org/10.1109/jeds.2021.3082420

[20] Şen, M., Özcan, M., & Eker, Y. R. (2024). A review on the lithium-ion battery problems used in electric vehicles. Next Sustainability, 3, 100036. doi: https://doi.org/10.1016/j.nxsust.2024.100036

[21] Misenan, M., & Khiar, A. (2023). Optimization of methyl cellulose biopolymer electrolyte conductivity via response surface methodology. Next Materials, 3, 100089 doi: https://doi.org/10.1016/j.nxmate.2023.100089

[22] Han, T., Chen, S., Yang, S., Song, T., Lin, X., Yu, Q., Han, D., Bobacka, J., & Niu, L. (2025). Determination of silver ions in distilled water by stripping voltammetry at a Nafion-coated gold electrode in combination with quartz crystal microbalance and electrochemical impedance spectroscopy. Talanta, 282, 127006. doi: https://doi.org/10.1016/j.talanta.2024.127006

[23] Goodson, M., & Guggilla, P. (n.d.). Investigation of Uv-Vis Characteristics of Pure/Doped Polystyrene Thin Films Prepared by Solution Casting Method Journal of Materials and Polymer Science.

[24] Baranwal, J., Barse, B., Fais, A., Delogu, G. L., & Kumar, A. (2022). Biopolymer: A Sustainable Material for Food and Medical Applications. In *Polymers* (Vol. 14, Issue 5). MDPI. doi: https://doi.org/10.3390/polym14050983

[25] Ndruru, S. T. C. L., Wahyuningrum, D., Bundjali, B., & Arcana, I. M. (2020). Preparation and characterization of biopolymer electrolyte membranes based on LiCLO4-Complexed methyl cellulose as lithium-ion battery separator. Journal of Engineering and Technological Sciences, 52(1), 28–50. doi: https://doi.org/10.5614/j.eng.technol.sci.2020.52.1.3

[26] Aziz, S. B., Asnawi, A. S. F. M., Kadir, M. F. Z., Alshehri, S. M., Ahamad, T., Yusof, Y. M., & Hadi, J. M. (2021). Structural, electrical and electrochemical properties of glycerolized biopolymers based on chitosan (Cs): Methylcellulose (mc) for energy storage application. Polymers, 13(8). doi: https://doi.org/10.3390/polym13081183

[27] Al-Saeedi, S. I., Aziz, S. B., Hadi, J. M., Hama, P. O., Abdulwahid, R. T., Abdalrahman, A. A., Murad, A. R., Karim, W. O., Abdul Halim, N., Fakhrul Zamani Kadir, M., & Hamad, S. M. (2023). Green biopolymer and plasticizer for solid electrolyte preparation: FTIR, electrochemical properties and EDLC characteristics. Arabian Journal of Chemistry, 16(9). doi: https://doi.org/10.1016/j.arabjc.2023.105046

[28] Sundermann, D. A., Park, B., Hirschberg, V., Schaefer, J. L., & Théato, P. (2023). Magnesium Polymer Electrolytes Based on the Polycarbonate Poly(2-butyl-2-ethyltrimethylene-carbonate). ACS Omega, 8(26), 23510–23520. doi: https://doi.org/10.1021/acsomega.3c00761

[29] Shiga, T., Kato, Y., & Inoue, M. (2021). Electrochemical Film Formation on Magnesium Metal in an Ionic Liquid That Dissolves Metal Triflate and Its Application to an Active Material with Anion Charge Carrier. ACS Applied Materials & Interfaces, 8(45), 30933–30940. doi: https://doi.org/10.1021/acsami.6b10107